# Rigorous Models for the Lorenz Equations

Warwick Tucker

December 6, 1996

**Abstract**

Inspired by numerical solutions of the Lorenz equations, we model the Poincaré map of the flow by a one-parameter map of the unit interval. For a certain region in the parameter space of the Lorenz equations, we show that the corresponding one-dimensional map is chaotic, imposing only minimal conditions on its derivative. Perturbing the map, we get a two-dimensional map corresponding to a flow in three dimensions. We show that the chaotic property is preserved under certain perturbations.

## Contents

# 1 Preliminaries

## 1.1 Global and Local Bifurcations

The Lorenz equations,

$$\dot{x} = -\sigma x + \sigma y$$
$$\dot{y} = rx - y - xz$$
$$\dot{z} = -bz + xy,$$

were introduced 1963 by E.N. Lorenz [6]. As a crude model of atmospheric dynamics, these equations led Lorenz to the discovery of sensitive dependence of initial values - an essential factor of unpredictability in meteorology. Later, it was to become one of the corner-stones in the theory of chaotic dynamical systems, and is also, more poetically, known as the *butterfly effect*.

Numerical simulations for parameter values $\sigma \approx 10, b \approx 8/3$ and $0 < r < \infty$ indicate that these equations exhibit a strange attractor for an open interval of $r$-values. However, this has not yet been rigorously proved. In this chapter we will see how the solutions change on a global scale as $r$ is varied. This gives us a rough idea of how the chaotic motion is created and destroyed. It also enables us to make an intelligent guess where to focus our attention when it comes to understanding the underlying mechanism of the system.

For $r < 1$, the origin is the only fixed point of the system, and it is a global sink (all three eigenvalues are real and negative).

At $r = 1$, there is a pitchfork bifurcation of fixed points, and for $r > 1$ there are three fixed points: the origin and a symmetric pair of stable fixed points, $C^{\pm} = (\pm\sqrt{b(r-1)}, \pm\sqrt{b(r-1)}, r-1)$. In the creation of $C^{\pm}$, the origin loses its stability.

Initially, the symmetric fixed points are sinks, but for $r$ slightly larger than one, two of the negative real eigenvalues become a complex conjugate pair: $C^{\pm}$ have turned into stable saddles. The unstable manifold of the origin, denoted $W^u(0)$, has two branches: one with $x > 0$ ($W^u_+(0)$) and one with $x < 0$ ($W^u_-(0)$. At this stage, $W^u_+(0)$ is attracted to and spirals towards $C^+$, and $W^u_-(0)$ is attracted to and spirals towards $C^-$, see Figure 1.a.

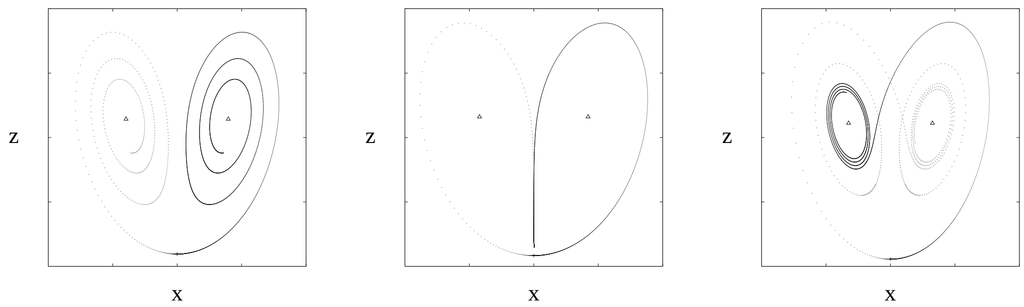


Figure 1: The Lorenz flow for (a) $r < r_{hom}$, (b) $r = r_{hom}$ and (c) $r > r_{hom}$.

At $r = r_{hom} \approx 13.926$, $W^u_+(0)$ makes such a large spiral around $C^+$ that it actually hits the stable manifold of itself, $W^s(0)$. As a consequence, we have a homoclinic orbit. By symmetry, we have a pair of homoclinic orbits, see Figure 1.b.

Although it seems intuitively clear, an analytic proof of the existence of these homoclinic orbits was presented as late as 1992 by Hasting and Troy, see [5]. They showed that for $\sigma = 10$ and $b = 1$, there exists a pair of homoclinic orbits for some $r \in (1, 1000)$.

Palis and Takens have in [10] rigorously studied homoclinic bifurcations, and it is clear that very complicated sets of closed orbits are created as $r$ is increased beyond $r_{hom}$. Numerical simulations indicate that the branches of $W^u(0)$ change side before spiraling in towards the fixed points $C^{\pm}$.

This results in the creation of two unstable closed orbits and a horseshoe. In 1995, Mischaikow and Mrozek [8] showed that for $(\sigma, b, r) \approx (45, 10, 54)$, the Lorenz equations do indeed contain a horseshoe. As the horseshoe is a trademark for chaos, it follows that the Lorenz equations are chaotic for these parameter values. However, the chaotic set (the horseshoe) is not attracting and it has measure zero, whereas the strange attractor mentioned above seems to be both attracting and large.

At $r = r_{het} \approx 24.06$, the branches of $W^u(0)$ become tangent to the stable manifolds of the two unstable closed orbits, see Figure 2.a, thus giving rise to a pair of heteroclinic orbits. This means that both branches wrap around the unstable closed orbits forever, which suggests that we may have an attracting invariant set. We will return to the breaking of this situation in the next chapter as it turns out to be a very suitable bifurcation for our needs.

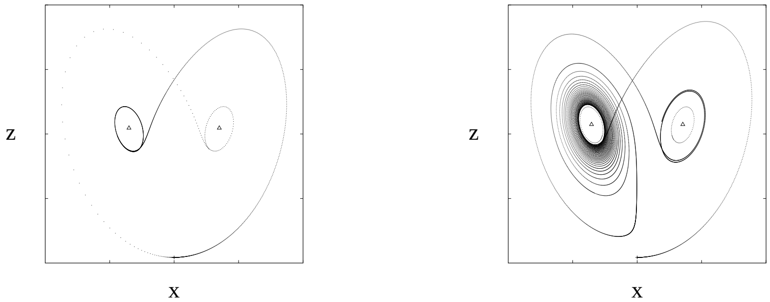


Figure 2: The Lorenz flow for (a) $r = r_{het}$, (b) $r > r_{het}$.

For $r > r_{het}$, the branches of $W^u(0)$ spiral outwards from the two unstable closed orbits. When the spirals reach a critical size, they cross over and start to spiral around the other fixed point. This seems to go on for ever.

At $r = r_H \approx 24.74$, the two unstable closed orbits shrink into $C^{\pm}$. The real parts of the complex conjugate eigenvalues of $C^{\pm}$ cross the imaginary axis and become positive as $r > r_H$. This is known as a Hopf bifurcation, and results in $C^{\pm}$ losing their stability, which leaves us with three unstable fixed points.

For $r$-values greater than roughly 31, there seems to appear intervals where we have stable closed orbits, and for $r \geq 200$ it has been proved in [12] that all solutions tend to a single closed orbit.

We end this introductory chapter with a bifurcation diagram illustrating some of the events described above.

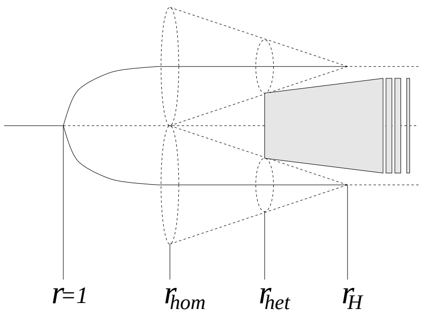


Figure 3: A bifurcation diagram for $r \in (0, 32)$. Numerical simulations indicate the presence of a strange attractor in the shaded region.

# 2 The One-Dimensional Case

## 2.1 Introduction

The Lorenz equations have inspired the study of iterated singular maps of the interval. These maps have their origin in the Poincaré map of the flow. In reality, the Poincaré map is two-dimensional, but due to the strong dissipative effects of the flow the map is "close" to a one-dimensional map. Naturally, we lose some information by this approximation, but a lot remains. The reduction makes it easier to study some qualitative features of the map. The idea is then to "thicken" the one-dimensional map via a perturbation so that we regain a two-dimensional map close to the original Poincaré map. This we do in chapter 3.

A reasonable demand on the one-dimensional map is that it should be chaotic. If this is not the case, one can hardly expect the perturbed two-dimensional map to have that feature. As long as the derivative of the map is greater than one, we have a uniformly expanding situation, which guarantees positive Lyapunov exponents. Breaking this condition, we can not a priori know if this feature is preserved. Furthermore, the presence of a discontinuity opposes a threat to topological transitivity, as iterated intervals may be cut in half when passing it. We show that, for a whole interval of parameters, the maps in our family are indeed chaotic.

This paper is inspired by the work of S. Luzzatto and M. Viana [7]. The bifurcation we study is simpler in the sense that we consider a perturbation of a map having a pair of symmetric fixed points, assuring that the derivative of the perturbed map can not be much less than one. On the other hand, we can prove that the map is topologically transitive without any extra assumptions on its derivative and we do not have to deal with any parameter exclusions. Furthermore, we do not require that the derivative tends to infinity at the discontinuity. This enables us to prove our results for a very large class of maps, strictly containing the Lorenz-like maps, as defined below.

## 2.2 Definitions

**Definition 2.1** *Consider a map, $f\colon I \to I$, where $I$ is any compact interval. For all $x \in I$ we define the Lyapunov exponent of $x$, $L(f,x)$, to be*

$$L(f,x) = \limsup_{n\to\infty} \frac{1}{n} \log |(f^n)'(x)|,$$

*where $f^n$ denotes the n:th iterate of $f$.*

A positive Lyapunov exponent of $x$ corresponds to an exponential average local expansion of points near $x$, i.e. $|f^n(x) - f^n(y)| \sim e^{nL(f,x)}$ for $y$ near $x$. If $L(f,x)$ is positive for a.e. $x \in I$, we say that $f$ is *Lyapunov chaotic* on $I$. A map that is Lyapunov chaotic can clearly not have any stable closed orbits. Although the functions we will be considering have a discontinuity, they are smooth elsewhere, and we can still talk about the Lyapunov exponent of a.e. $x$.

**Definition 2.2** *Consider a map, $f\colon I \to I$, where $I$ is any compact interval. $f$ is topologically transitive on $I$ if, for any two open subsets, $U, V \subset I$, there exists $n > 0$ such that $f^n(U) \cap V \neq \emptyset$.*

Hence, a map, $f$, which is topologically transitive on $I$ cannot have two disjoint open nonempty $f$-invariant sets in $I$. This guarantees that almost all points are "mixed" under iterations of $f$. In fact, our definition is equivalent to saying that there exists a dense orbit in $I$.

**Definition 2.3** *Consider a map, $f\colon I \to I$, where $I$ is any compact interval. $f$ is chaotic on $I$ if*

*(1) $I$ is forward invariant ($f(I) = I$),*

*(2) $f|_I$ is Lyapunov chaotic,*

*(3) $f|_I$ is topologically transitive.*

### 2.3 The Poincaré Map of the Lorenz Flow

By a simple change of variables, the Lorenz equations can be put in their Jordan normal form

$$\begin{aligned}\dot{x} &= \lambda_u x - k_1(x+y)z\\ \dot{y} &= \lambda_{ss} y + k_1(x+y)z\\ \dot{z} &= \lambda_s z + (x+y)(k_2 x + k_3 y),\end{aligned}$$

where $k_1, k_2$ and $k_3$ only depend on the parameters $\sigma, b$ and $r$. If the eigenvalues at a fixed point satisfy certain non-resonance conditions, we can find linearizing coordinates for a neighbourhood of the fixed point.

**Definition 2.4** *The eigenvalues $\lambda_1, \ldots, \lambda_n$ are resonant if there exists $m_k \in \mathbb{N}$ with $|m| = \sum_{k=1}^n m_k \geq 2$ such that*

$$\sum_{k=1}^{n} m_k \lambda_k = \lambda_i$$

*for some $i = 1, \ldots, n$. $|m|$ is called the order of resonance.*

We can now state an extension of the Grobman-Hartman theorem, due to Sternberg [9]:

**Theorem 2.5** *If the eigenvalues $\lambda_1, \ldots, \lambda_n$ of the linear part of a $C^\infty$ vector field at a fixed point are non-resonant, then there exists a $C^\infty$ change of coordinates in a neighbourhood of the fixed point which brings the differential equation into linear form.*

A milder version of this theorem is due to Belitskii [2]:

**Theorem 2.6** *If the eigenvalues $\lambda_1, \ldots, \lambda_n$ of the linear part of a $C^{(1,1)}$ vector field at a fixed point satisfy $\Re(\lambda_i) \neq \Re(\lambda_j) + \Re(\lambda_k)$, when $\Re(\lambda_j) < 0 < \Re(\lambda_k)$, then there exists a $C^1$ change of coordinates in a neighbourhood of the fixed point which brings the differential equation into linear form.*

Here $\Re(x)$ denotes the real part of $x$, and $C^{(1,1)}$ is the set of all functions having Lipschitz first derivatives. Note that $C^2 \subset C^{(1,1)} \subset C^1$.

As the Lorenz equations are given by an analytic vector field, and as we want to linearize the flow in a neighbourhood of the origin where all eigenvalues are real, the conditions in the theorem above are satisfied if

$$\lambda_{ss} < \lambda_s < 0 < \lambda_u, \quad |\lambda_s| < \lambda_u < |\lambda_{ss}| \quad \text{and} \quad \lambda_s \neq \lambda_{ss} + \lambda_u.$$

Assuming that these conditions hold, we can make a smooth change of coordinates which linearizes the flow in a neighbourhood, $\mathcal{U}$, of the origin. The linear flow in $\mathcal{U}$ is given by

$$\psi(x, y, z, t) = (xe^{\lambda_u t}, ye^{\lambda_{ss} t}, ze^{\lambda_s t}).$$

Inside $\mathcal{U}$ we will focus on a small cube $\mathcal{Q}$ with side length $2h$. We denote the cube's lid by $\Sigma$ and its two sides by $\Sigma^+$ and $\Sigma^-$ (see Figure 4). Taking $\Sigma$ as the Poincaré section, the flow can be decomposed into two different parts: one part flowing inside $\mathcal{Q}$ and one part outside.

We start with the first part. As it is inside $\mathcal{Q}$, we can use the linearizing coordinates. This induces two maps: $R_0^\pm : \Sigma \to \Sigma^\pm$, where

$$R_0^+(x, y, h) = (h, y(\frac{x}{h})^{-\frac{\lambda_{ss}}{\lambda_u}}, h(\frac{x}{h})^{-\frac{\lambda_s}{\lambda_u}})$$

is defined for $x > 0$ and

$$R_0^-(x, y, h) = (-h, y(\frac{|x|}{h})^{-\frac{\lambda_{ss}}{\lambda_u}}, h(\frac{|x|}{h})^{-\frac{\lambda_s}{\lambda_u}})$$

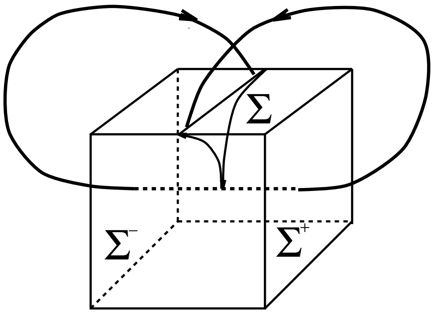


Figure 4: The global flow inside and outside the cube.

is defined for $x < 0$. These two functions can be merged, and setting $\mu = -\frac{\lambda_{ss}}{\lambda_u}$ and $\nu = -\frac{\lambda_s}{\lambda_u}$ gives $R_0\colon \Sigma \to \Sigma^+ \cup \Sigma^-$, where

$$R_0(x, y, h) = (\operatorname{sgn}(x)h, y(\frac{|x|}{h})^\mu, h(\frac{|x|}{h})^\nu).$$

Note that $R_0$ is not defined for $x = 0$. This line corresponds to the stable manifold of the origin - a point that hits this set tends to the origin and will never return to $\Sigma$.

Continuing from $\Sigma^\pm$ back to $\Sigma$, the flow leaves $\mathcal{U}$. Outside this neighbourhood we do not know exactly how the flow behaves, but we can make an approximation. To lowest order $R_1^\pm\colon \Sigma^\pm \to \Sigma$ can be taken to be affine, so assuming that $c_1c_4 - c_2c_3 \neq 0$ we have

$$R_1^+(h, y, z) = (a + c_1y + c_2z, b + c_3y + c_4z, h)$$

and

$$R_1^-(-h, y, z) = (-a + c_1y - c_2z, -b + c_3y - c_4z, h).$$

Combining these two functions gives $R_1\colon \Sigma^+ \cup \Sigma^- \to \Sigma$, where

$$R_1(h, y, z) = (\operatorname{sgn}(h)(a + c_2z) + c_1y, \operatorname{sgn}(h)(b + c_4z) + c_3y, |h|).$$

It is this function that corresponds to the global behavior of the flow. Changing the parameters will not qualitatively change of $R_0$, but may have serious effects on $R_1$. As an example, we recall from the introductory section that, given $\sigma$ and $b$, there exists an $r$-value $r_{hom}$ such that for $r = r_{hom}$, the branches of the unstable manifold of the origin, $W^u(0)$, intersect the stable manifold, $W^s(0)$, non-transversally. This gives a symmetric pair of homoclinic orbits. Changing the parameter $r$, the global flow acts very differently depending on $\operatorname{sgn}(r - r_{hom})$, whereas $R_0$ hardly changes at all.

If we compose $R_0$ and $R_1$, re-scale and drop the dummy variable, we get an approximate global Poincaré map $R = R_1 \circ R_0\colon S(\Sigma) \to S(\Sigma)$, where

$$R(x, y) = (\operatorname{sgn}(x)(d_1|x|^\nu - a) + d_2y|x|^\mu, \operatorname{sgn}(x)(d_3|x|^\nu - b) + d_4y|x|^\mu).$$

Since $\nu < 1 < \mu$, the $x$-coordinate can be decoupled into a one-dimensional map:

$$P_a(x) = \operatorname{sgn}(x)(d|x|^\nu - a).$$

If $d > 0$, this map is valid as an approximate model of the projected flow near the homoclinic orbits if $a$ and $|x|$ are small. This fact motivates our study of discontinuous maps of the interval.

## 2.4 Discontinuous Maps

We will now model the return map corresponding to the projection of the Lorenz flow by a one-dimensional map depending on a parameter $a$. In fact, we will consider a much larger family of maps, strictly containing the *Lorenz-like* maps, as defined below.

Set $\Lambda_a = [-a, a]$, and consider $f_a : \Lambda_a \to \mathbb{R}$, where $f_a$ is defined as follows:

$$f_a(x) = \operatorname{sgn}(x)(f(|x|) - a) \qquad (x \neq 0)$$

where for all $x > 0$, $f(x)$ is smooth and satisfies:

**L1:** $f(0) = 0$, and $f'(0) > 0$,

**L2:** $f''(x) < 0$ for all $x > 0$,

**L3:** $f(c) = 2c$ for some $c > 0$,

**L4:** $f'(c) \geq 1$.

We now list some useful consequences of **L1-L4**.

**C1:** For $a \geq c$ we have $f_a(\Lambda_a) = \Lambda_a$ ($\Lambda_a$ is forward invariant).

**C2:** $f'(c) \in [1, 2)$ and $f'(0^+) \in (2, \infty]$.

**C3:** For $a > c$ we have $f_a(a) < a$ (a finite maximal number of iterations per leap), and for $a \approx c$, we have $f_a'(f_a(a)) > 1$ (at most one contractive iteration per leap).

A *leap* takes place when an iterate changes branch of the graph.
By strengthening the requirements as follows:

**GL1:** $f(x) = \kappa x^\nu + o(x^\nu)$, where $\kappa > 0$ and $\nu \in (0, 1)$,

**GL2:** the same as **L2**,

**GL3:** the same as **L3**,

**GL4:** $f'(x) \geq \sqrt{2}$,

we get a smaller class of maps, called geometric *Lorenz-like* maps. This class of maps was used in early attempts to model the behaviour of the Lorenz flow. However, computer simulations indicate that condition **GL4** does not hold. This is why we study the larger class of maps, satisfying **L1-L4**.
**Example:** By taking $f(x) = x^\nu + x^{2\nu}$ and $\nu = \frac{1}{3}$, the conditions **GL1-GL3** and **L4** are fulfilled with $c = 1$ and $f_c'(c) = 1$. We get the following function (see Figure 5):

$$f_a(x) = \operatorname{sgn}(x)(|x|^{\frac{1}{3}} + |x|^{\frac{2}{3}} - a).$$

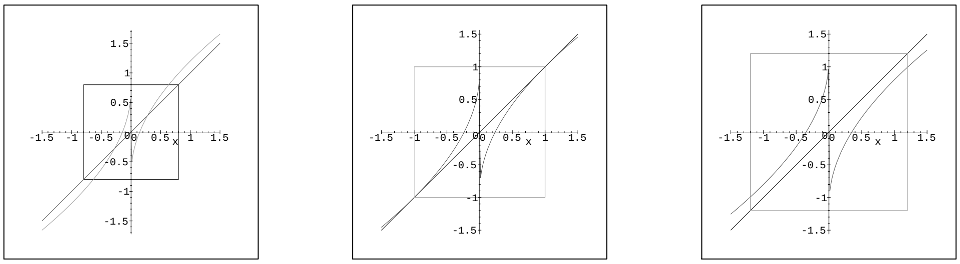

Figure 5: The function $f_a(x)$ with (a) $a < c$, (b) $a = c$ and (c) $a > c$.

We now claim that, given any $f_a$ satisfying **L1-L4**, there exists $\epsilon > 0$ such that for all $a \in [c, c+\epsilon]$, $f_a$ is chaotic. It is proved that, although we lose expansiveness at the parts of an orbit where the derivatives are small, the gain near the discontinuity compensates for this. The main idea is then to use properties of the map which are unique for the bifurcation we will be considering, allowing us to make the area where large derivatives are needed arbitrarily small. The points that do not have positive Lyapunov exponents are exactly the pre-images of 0. We denote this set $\mathcal{Z}_a$. Note that $\mathcal{Z}_a$ is countable, and hence has measure zero.

## 2.5 Results

**Theorem 2.7** *Suppose $f_a$ satisfies **L1-L4**. Then there exists $\epsilon > 0$ such that for all $a \in [c, c+\epsilon]$, $f_a$ is chaotic on $\Lambda_a$.*

We will prove this theorem in the next section.

**Remark:** Consider any candidate, $P_a$, for a Poincaré map of the Lorenz flow. The invariant set created as $a$ becomes positive is unstable and the situations looks like Figure 5.a. For the set to become attracting we need $P_a$ to have a trapping region containing the origin. Thus we must have a similar situation as in Figure 5.b. In the case of the Lorenz equations, this corresponds to $r = r_{het}$. As computer simulations show that a Hopf bifurcation takes place after $\Lambda_a$ becomes forward invariant, i.e. $r_H > r_{het}$, we will have $P_c'(c) > 1$ (the case $P_c'(c) = 1$ corresponds to the Hopf bifurcation taking place just as $\Lambda_a$ becomes invariant, i.e. $r_H = r_{het}$). It follows that there exists $\epsilon > 0$ such that $P_a'(a) > 1$ for all $a \in [c, c+\epsilon]$. In [4], [11], [13] and [15] it is assumed that $P_a'(a) > \sqrt{2}$ for all $a \in [c, c+\epsilon]$. However, these articles treat a situation corresponding to a different range of parameters which makes this assumption on the derivative necessary to ensure that $P_a|_{\Lambda_a}$ is eventually onto, and hence topologically transitive. By necessary, we mean in the sense that a weakening of the condition, like $P_a'(a) > \alpha$, $\alpha < \sqrt{2}$, will not always give chaotic maps, see [14]. However, we study a special bifurcation, and it follows from our theorem that in our case this assumption is superfluous. Since we must have $P_c'(c) \geq 1$ by simple geometrical reasons, our theorem assures us that $P_a$ is chaotic on $\Lambda_a$ even if $P_c'(c) < \sqrt{2}$, which seems to be the case with the Lorenz flow. As the map is chaotic for a whole interval of parameter values, the possibility of using computers for further investigations is not excluded.

## 2.6 Proof of the Theorem

We will start by dealing with the case $a > c$. The case $a = c$ will then be proved by slightly modifying the proofs already used. We proceed in this manner to avoid getting stuck into irrelevant details. In order to make the proof easy to follow, we split the theorem into two parts: in Proposition 2.12 we prove that $f_a$ is Lyapunov chaotic and in Proposition 2.14 we prove that $f_a$ is topologically transitive. Also, we will assume that $f_c'(c) = 1$ as this is the worst case of condition **L4**.

First, we need to state a few trivial lemmas. Fix a small and positive $\delta$.

**Lemma 2.8** *For all $x$ near 0,*
*(1) $2x \leq f_a(x) + a$, if $x > 0$,*
*(2) $2x \geq f_a(x) - a$, if $x < 0$,*
*(3) $2 \leq f_a'(x)$.*

**Lemma 2.9** *For all $x$ near $c$ or $-c$, $|f_a'(x) - 1| \leq \delta$.*

These two lemmas follow immediately from **L1-L3** plus the assumption $f_c'(c) = 1$, respectively. We shall always make sure that the lemmas are valid for all $x$ in a $2\epsilon$-neighbourhood of $\{-c, 0, c\}$ by taking $\epsilon$ small enough. As a direct result from Lemma 2.8, we have:

**Lemma 2.10** *For all $\epsilon > 0$ and $\theta = \theta(\epsilon) > 0$ sufficiently small,*
*(1)* $-\frac{\epsilon+\theta}{2} \leq f_{c+\epsilon}^{-1}(c-\theta)$,
*(2)* $\frac{\epsilon+\theta}{2} \leq f_{c+\epsilon}^{-1}(-c+\theta)$.

*Proof.* We only prove (1) since the proof of (2) is analogous. By Lemma 2.8, we have

$$2f_{c+\epsilon}^{-1}(c-\theta) \geq f_{c+\epsilon}(f_{c+\epsilon}^{-1}(c-\theta)) - (c+\epsilon) = -(\epsilon+\theta),$$

which directly gives the desired result. □

The point of this lemma is that the pre-image of a neighbourhood of $c$ is relatively small since $\lim_{x\to 0} f_a'(x) > 2$. This is exactly what we need to ensure that before an iterate enters the contractive area, it has been very close to the discontinuity. In fact, it has been close enough to compensate the contraction.

**Proposition 2.11** *If $a \in (c, c+\epsilon)$ and $\epsilon$ is small enough, there exists $\alpha > 0$ such that*

$$(f_a^n)'(x) \geq \min\{e^\alpha, f_a'(x)\}e^{\alpha(n-1)},$$

*for all $x \in \Lambda_a$ such that $f_a^k(x) \neq 0$ for $k = 0, 1, ..., n-1$.*

*Proof.* The proposition is trivial if $f'(c) > 1$, so assume that $f'(c) = 1$. We will prove the proposition by induction. It is clearly true for $k = 0$, so assume the proposition holds up to step $n$. Given $\theta$ and $\epsilon$, both positive and small, there exists $\alpha > 0$ such that if $f_{c+\epsilon}^n(x) \in \Lambda_{c-\theta}$, the derivative at the point $f_{c+\epsilon}^n(x)$ is greater than $e^\alpha$, i.e.

$$f_{c+\epsilon}'(f_{c+\epsilon}^n(x)) > e^\alpha.$$

Bearing this in mind, we may assume that

$$f_{c+\epsilon}^n(x) \in \Lambda_{c+\epsilon} \setminus \Lambda_{c-\theta}.$$

Taking $\epsilon$ and $\theta$ small will, by Lemma 2.10, ensure that

$$f_{c+\epsilon}^{n-1}(x) \in (-\frac{\epsilon+\theta}{2}, 0),$$

which is close to the discontinuity. By Lemmas 2.8 and 2.9, we can clearly take $\epsilon$ and $\theta$ small enough to have

$$f_{c+\epsilon}'(f_{c+\epsilon}^{n-1}(x)) > \frac{3}{2}e^\alpha \quad \text{and} \quad f_{c+\epsilon}'(f_{c+\epsilon}^n(x)) > \frac{2}{3}e^\alpha,$$

for all $x$ such that $f_{c+\epsilon}^n(x) \in \Lambda_{c+\epsilon} \setminus \Lambda_{c-\theta}$. Combining these inequalities, we get

$$(f_{c+\epsilon}^2)'(f_{c+\epsilon}^{n-1}(x)) = f_{c+\epsilon}'(f_{c+\epsilon}^{n-1}(x))f_{c+\epsilon}'(f_{c+\epsilon}^n(x)) > \frac{3}{2}e^\alpha\frac{2}{3}e^\alpha = e^{2\alpha}.$$

This completes the proof. □

**Proposition 2.12** *Suppose $f_a$ satisfies **L1-L4**. Then there exists $\epsilon > 0$ such that $f_a$ is Lyapunov chaotic for all $a \in (c, c+\epsilon)$.*

*Proof.* Take $x \in \Lambda_a \setminus \mathcal{Z}_a$. Then, by Proposition 2.11,

$$\begin{aligned} L(f_a, x) &= \limsup_{n\to\infty} \frac{1}{n} \log|(f_a^n)'(x)| \\ &\geq \limsup_{n\to\infty} \frac{1}{n} \min\{n\alpha, (n-1)\alpha + \log|f_a'(x)|\} \\ &= \limsup_{n\to\infty} \min\{\alpha, \frac{n-1}{n}\alpha + \frac{1}{n}\log|f_a'(x)|\} \\ &= \alpha > 0. \end{aligned}$$

Since the measure of $\mathcal{Z}_a$ is zero, the proof is complete. □

**Corollary 2.13** *$\mathcal{Z}_a$ is dense in $\Lambda_a$ for all $a \in (c, c+\epsilon)$.*

*Proof.* Suppose $\mathcal{Z}_a$ is not dense in $\Lambda_a$. Then there exists an open set $B \subset \Lambda_a \setminus \mathcal{Z}_a$. By Proposition 2.11, $|f_a^n(B)|$ is eventually exponentially increasing with $n$, which leads to a contradiction, since we must have $|f_a^n(B)| \leq |f_a^n(\Lambda_a)| = |\Lambda_a| = 2a$. □

What now remains is to prove topological transitivity. The difficulty is that when iterating an interval, it can be cut in half as it passes the discontinuity. This is overcome by making sure that immediately after such a slicing, the two segments are more than doubled in lenghts.

**Proposition 2.14** *Suppose $f_a$ satisfies **L1-L4**. Then there exists $\epsilon > 0$ such that $f_a|_{\Lambda_a}$ is topologically transitive for all $a \in (c, c+\epsilon)$.*

*Proof.* Throughout the proof, let $a = c + \epsilon$. Recall the final inequality in the proof of Proposition 2.11:

$$(f_a^2)'(f_a^{n-1}(x)) = f_a'(f_a^{n-1}(x))f_a'(f_a^n(x)) > e^{2\alpha}.$$

This holds when $f_a^{n-1}(x) \in (f_a^{-1}(c-\theta), f_a^{-1}(a))$ or, by symmetry, when

$$f_a^{n-1}(x) \in f_a^{-1}(\Lambda_a \setminus \Lambda_{c-\theta}).$$

As any iterate of an interval may be cut in half by the discontinuity when intersecting the set $f_a^{-1}(\Lambda_a \setminus \Lambda_{c-\theta})$, we want to ensure that $e^{2\alpha} \geq \beta > 2$. This is easily achieved if we can take $\epsilon$ and $\theta$ small. However, we cannot take $\theta$ too small compared to $\epsilon$, since we also must make sure that both connected components of $f_a^{-1}(\Lambda_a \setminus \Lambda_{c-\theta})$ cover "good" domains. By a good domain, we mean a connected set, $E \subset \Lambda_a$, such that we have

$$f_a(E) \cap E \neq \emptyset.$$

This is achieved by choosing $\theta$ such that $(f_a^2(0^-), f_a(0^-)) \subset (c-\theta, a)$, which reduces to making sure that $c - \theta \leq f_a(a)$. By the definition of $f_a$, and using the facts that $f_c(c) = c$ and $f_c'(c) < 2$, we get $f_a(a) > c - \epsilon$, so we can take $\theta = \epsilon$.

We now claim that any interval, $U \subset \Lambda_a$, will eventually be mapped onto $\Lambda_a$. As a consequence, we will also have topological transitivity. By symmetry, it is enough to show that there exists $n > 0$ such that $f_a^n(U) \supset (f_a^{-1}(c-\epsilon), 0)$, since then $f_a^{n+1}(U) \supset (c-\epsilon, a) \supset (f_a(a), a)$. Hence

$$\bigcup_{k=1}^{N} f_a^{n+k}(U) \supset \bigcup_{k=1}^{N} (f_a^k(a), f_a^{k-1}(a))$$

will intersect every open set in $\Lambda_a$ for some finite $N$. This is easily seen by noting that there exists $M$ such that $0 \in (f_a^M(a), f_a^{M-1}(a))$. This means that $(-a, 0) \subset (f_a^M(a), f_a^{M-1}(a)) \cup (f_a^{M+1}(a), f_a^M(a))$, and we only need one more iterate to cover $\Lambda_a \setminus \{-a, a\}$ (see Figure 6).

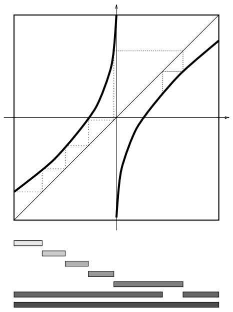

Figure 6: Iterates of $f_a(U)$.

We now have to prove that there really exists $n > 0$ such that

$$f_a^n(U) \supset (f_a^{-1}(c-\epsilon), 0).$$

By Corollary 2.13, we have $\mathcal{Z}_a \cap U \neq \emptyset$. Hence we may assume that $U \subset (f_a^{-1}(c-\epsilon), f_a^{-1}(-c+\epsilon))$, since it will intersect that part of $\Lambda_a$ sooner or later. We start off by setting $U_0$ as the largest component of $U \setminus \{0\}$. ($U_1$ is the largest component of the next intersection with $\{0\}$ and so on.) As long as the iterates $f_a^n(U_0)$ do not hit $\{0\}$, everything is fine since $|f_a^n(U_0)|$ is eventually exponentially increasing by Proposition 2.11. When $\{0\} \in f_a^n(U_0)$, $f_a^n(U_0)$ is cut, possibly in half. Thanks to our choice of $\theta$, both components of $f_a^n(U_0) \setminus \{0\}$ will be stretched by a factor $\beta$, which is greater than two. Continuing the procedure with the largest component ensures that we still have an exponentially increasing sequence, since inductively

$$|U_i| \geq \frac{\beta}{2}|U_{i-1}| \geq (\frac{\beta}{2})^i |U_0|.$$

As a consequence, $U_i$ will eventually cover one of the components of $(f_a^{-1}(c-\epsilon), f_a^{-1}(-c+\epsilon)) \setminus \{0\}$, which by symmetry completes the proof. □

We conclude this section by discussing the proof of the theorem when $a = c$. The only real change is that the map $f_c$ has two fixed points, $c$ and $-c$. As a consequence an orbit can have any number of iterations before a leap. On the other hand, the derivative is greater than one, except at the two fixed points. Thus we have no contraction whatsoever. Another bonus is that we may choose $\theta$ arbitrarily small. Using these facts, the proofs of propositions 2.11 and 2.14 are immediate. We therefore omit the details and consider the proof complete for $a \in [c, c+\epsilon]$.

**Remark:** Note that we have in fact proved that $f_a$ is *locally eventually onto*, i.e. any open set will eventually be mapped onto the whole interval $\Lambda_a$. This is a stronger condition than being topologically transitive, and we can not achieve this in the two-dimensional case.

# 3 The Two-Dimensional Case

## 3.1 Definitions and Results

In the previous chapter we proved that the one-dimensional map, $f_a$, was chaotic on the interval $\Lambda_a$. We now want to "thicken" the map $f_a(x)$, thus making it two-dimensional. In the spirit of [1], we define a two-dimensional map, $R_{a,b}$, which should be viewed as a perturbation of a degenerate two-dimensional embedding of $f_a$. The map $R_{a,b}$ is defined on a compact rectangle, $N_{a,b}$, specified in Proposition 3.5. $N_{a,b}$ shrinks continuously to $\Lambda_a$ as $b \to 0$, so $\cap_{b>0} N_{a,b} = \Lambda_a$.

We start by embedding $f_a$ in two dimensions:

$$f_a(x) \to (f_a(x), 0).$$

Now we will define perturbations of the $x$- and $y$-components, by making them maps from $\mathbb{R}^2$ to $\mathbb{R}$. We start with $f_a$:

Consider all functions $F_a(x,y)\colon \mathbb{R}^2 \to \mathbb{R}$ having the following symmetry: $F_a(-x,-y) = -F_a(x,y)$. Set

$$r(y) = \max_{i=0,1} \sup_{(x,y)\in N_{a,b}} |\partial_x^i F_a(x,y) - \partial_x^i f_a(x)|.$$

We demand that $\lim_{y\to 0} r(y) = 0$ for all $(x,y) \in N_{a,b}$, and that $|\partial_y F_a|$ is at most proportional to $|\partial_x F_a|$, i.e.

$$|\partial_y F_a(x,y)| \le K |\partial_x F_a(x,y)|$$

for some $K > 0$ and for all $(x,y) \in N_{a,b}$. The discontinuity of $f_a$ will generate a whole line of discontinuities of $F_a$, which we denote $S_{a,b}$. In terms of Lorenz-like flows, this line corresponds to the intersection of the stable manifold of the origin and the the return plane under consideration.

We now turn to the $y$-component:

Consider all functions $G(x,y)\colon \mathbb{R}^2 \to \mathbb{R}$ which have the same symmetry as $F_a$. We demand that $0 < |G(x,y)| \le \hat{K}$ for all $(x,y) \in N_{a,b}$, that $G$ is continuous on both sides of $S_{a,b}$, and that $|\partial_x G|$ and $|\partial_y G|$ are at most proportional to $|\partial_x F_a|$. Finally, we set $G_b(x,y) = bG(x,y)$.

Combining these perturbations of the two-dimensional embedding gives us a true two-dimensional map:

$$f_a(x) \to (f_a(x), 0) \to (F_a(x,y), G_b(x,y)),$$

which defines our fully perturbed map.

**Definition 3.1** $R_{a,b}(x,y) = (F_a(x,y), G_b(x,y))$.

This definition is motivated by the fact that $R_{a,0}^n(x,0) = f_a^n(x)$, which we know is chaotic on $\Lambda_a$. The symmetry condition on $F$ and $G$ comes from the symmetry in the Lorenz equations. It is not a crucial condition, but it certainly makes the calculations more easy to follow. One reason for us not demanding smoothness of the perturbation in the $y$-variable of $F_a$ is that we want a situation similar to [1], where the one-dimensional map

$$f_a(x) = 1 - ax^2$$

is perturbed into the two-dimensional map

$$R_{a,b}(x,y) = (1 + y - ax^2, bx).$$

This gives us a larger class of admissible perturbations than if we only had considered $C^1$ perturbations of $f_a$.

The main result in this chapter is the following:

**Theorem 3.2** *For all $a \in (c, c+\epsilon)$, there exists $b_0 > 0$ such that for $b \in (0, b_0)$, $R_{a,b}$ is chaotic on $\mathcal{A}_{a,b}$, where $\mathcal{A}_{a,b} \subset \mathbb{R}^2$ has positive one-dimensional Lebesgue measure and is attracting.*

As we mentioned earlier, this theorem can be smoothly "glued" to the one-dimensional result since $b_0 \to 0$ when $\epsilon \to 0$.

**Example:** Consider the following map:

$$R_{a,b}(x,y) = \big(\mathrm{sgn}(x)(|x|^{\nu} + |x|^{2\nu} - a) + c_1 y|x|^{\eta}, b(\mathrm{sgn}(x)(c_2|x|^{\nu}+1) + c_3 y|x|^{\eta})\big),$$

where $a$ and $b$ are viewed as parameters and $c_i$, $\nu$ and $\eta$ are constants. Making the choice $c_1 = 0.01$, $c_2 = 3$, $c_3 = -0.05$, $\nu = \frac{1}{3}$ and $\eta = 1.8$, we get a map similar to the Poincaré map of the Lorenz flow. The pictures below illustrate the qualitative similarities between these two maps.

Figure 7: (a) Plot of $R_{a,b}$, (b) Poincaré map of the Lorenz flow

## 3.2 Trapping Regions

We will first show that there exists a trapping region for $R_{a,b}$, i.e. a region that is mapped into itself by $R_{a,b}$. This is a fundamental ingredient in the the definition of chaos.

**Definition 3.3** *A closed region $N \subset \mathbb{R}^2$ is a trapping region for $R$ if $R(N)$ is contained in the interior of $N$.*

**Definition 3.4** *A set $\mathcal{A}$ is called a transitive attractor for $R$ if $R$ is topologically transitive on $\mathcal{A}$ and if there exists a neighbourhood $U$ of $\mathcal{A}$ for which the closure of $U$ is a trapping region and*

$$\mathcal{A} = \bigcap_{n \geq 0} R^n(\bar{U}).$$

**Proposition 3.5** *For all $a \in (c, c+\epsilon)$ there exists $b_0 > 0$ such that for $b \in (0, b_0)$, $R_{a,b}$ has a trapping region, $N_{a,b}$.*

*Proof.* As $f_a \colon \Lambda_a \to \Lambda_a$, for all $a \in [c, c+\epsilon]$ it is obvious that

$$R_{a,0} \colon \Lambda_a \times \{0\} \to \Lambda_a \times \{0\}.$$

Being more thorough, one can prove that for $\delta \in [0,\epsilon]$, $f_{c+\delta} \colon \Lambda_{c+\frac{2}{\gamma}\delta} \to \Lambda_{c+\delta}$, where $\gamma = f_c'(c) \in [1,2)$. This fact is equivalent to the condition $f(c + \frac{2}{\gamma}\delta) < 2(c+\delta)$, which is proved as follows: by **L4**, we know that $f'(c) = \gamma \in [1,2)$, and by **L3** we have that $f(c) = 2c$. Condition **L2** then implies that $f(c+h) \leq 2c + \gamma h$, which gives the desired result by setting $h = 2\delta/\gamma$. Hence, for $\delta \in (0,\epsilon)$, $f_{c+\delta}$ is a strict contraction on $\Lambda_{c+\frac{2}{\gamma}\delta}$, which means that $R_{c+\delta,0}$ is a strict contraction on $\Lambda_{c+\frac{2}{\gamma}\delta} \times \{0\}$. As $F_a$ is continuous in the $y$-variable at the origin, a small perturbation in the $y$-variable of $F_{c+\delta}$ will not alter its image too much. Thus, if $\tilde{b}$ is sufficiently small, $R_{c+\delta,0}$ will remain a strict contraction on $\Lambda_{c+\frac{2}{\gamma}\delta} \times \Lambda_{\tilde{b}}$. Since we can make the image of $G_b$ arbitrarily small on bounded sets by taking $b$ small, we can find $b_0$ so that $G_{b_0}$ maps $\Lambda_{c+\frac{2}{\gamma}\delta} \times \Lambda_{\tilde{b}}$ strictly into $\Lambda_{\tilde{b}}$.

Setting $a = c + \delta$, this ensures that $R_{a,b}$ is a strict contraction on $\Lambda_{c+\frac{2}{\gamma}\delta} \times \Lambda_{\tilde{b}}$ for all $b \leq b_0$. As $\delta \in (0, \epsilon)$, we have a continuum of candidate trapping regions. Since it is of no importance which one we choose, we will refer to any one of these sets as $N_{a,b}$, with the demand that $N_{a,b}$ shrinks continuously to $\Lambda_a$ as $b \to 0$. □

The proposition tells us that the maps $R_{a,b}$ have trapping regions for a large set of parameters, in the sense of two-dimensional Lebesgue measure. We will now restrict our attention to the invariant set

$$\mathcal{A}_{a,b} = \bigcap_{n \geq 0} R^n_{a,b}(N_{a,b}).$$

## 3.3 Positive Lyapunov Exponents

Next, we want to prove that $R_{a,b}$ is Lyapunov chaotic on $\mathcal{A}_{a,b}$. To begin with, we will prove that $R_{a,b}$ is Lyapunov chaotic on $N_{a,b}$. This property strongly depends on the fact that certain horizontal cone fields are forward invariant under $DR_{a,b}$. Analogously to the one-dimensional case, we will show that the points that do not have positive Lyapunov exponents are exactly the points that eventually are mapped to the set of discontinuity, $S_{a,b}$. We denote this set $\mathcal{Z}_{a,b}$, i.e.

$$\mathcal{Z}_{a,b} = \{(x, y) \in N_{a,b} \colon R^n_{a,b}(x, y) \in S_{a,b} \text{ for some } n \geq 0\}.$$

Since $\mathcal{Z}_{a,b}$ has measure zero in the sense of two-dimensional Lebesgue measure, we will have proved that the map $R_{a,b}$ is Lyapunov chaotic on $N_{a,b}$.

**Proposition 3.6** *For all $a \in (c, c + \epsilon)$ there exists $b_0 > 0$ such that for $b \in (0, b_0)$, the cone field, $C(x, y) = \{(v_1, v_2) \in TN_{a,b}(x, y) \colon |v_2| \leq \sqrt{b}|v_1|\}$, is invariant under $DR_{a,b}$, i.e. $DR_{a,b}(x, y) \cdot C(x, y) \subset C(R_{a,b}(x, y))$.*

*Proof.* By the definition of $R_{a,b}$,

$$DR_{a,b}(x, y) = \begin{pmatrix} \partial_x F_a & \partial_y F_a \\ \partial_x G_b & \partial_y G_b \end{pmatrix} = \begin{pmatrix} \partial_x F_a & \partial_y F_a \\ b\partial_x G & b\partial_y G \end{pmatrix}.$$

Thus, assuming that $|v_2| \leq \sqrt{b}|v_1|$, we have

$$DR_{a,b}(x, y) \begin{pmatrix} 1 \\ \frac{v_2}{v_1} \end{pmatrix} = \begin{pmatrix} \partial_x F_a + \frac{v_2}{v_1}\partial_y F_a \\ b(\partial_x G + \frac{v_2}{v_1}\partial_y G) \end{pmatrix} = \begin{pmatrix} w_1 \\ w_2 \end{pmatrix}.$$

When restricted to the trapping region, $F_a$ and $G$ satisfy

$$|\partial_y F_a|, |\partial_x G|, |\partial_y G| \leq K|\partial_x F_a|.$$

Using this, we get

$$\begin{aligned} |w_1| &= |\partial_x F_a + \frac{v_2}{v_1}\partial_y F_a| \geq |\partial_x F_a| - \sqrt{b}|\partial_y F_a| \\ &\geq |\partial_x F_a| - K\sqrt{b}|\partial_x F_a| = |\partial_x F_a|(1 - K\sqrt{b}) \\ &\geq (1 - r(y))(1 - K\sqrt{b})f'_a(x), \end{aligned}$$

and

$$\begin{aligned} |w_2| &= |b(\partial_x G + \frac{v_2}{v_1}\partial_y G)| \leq b(|(\partial_x G| + \sqrt{b}|\partial_y G)|) \\ &\leq b(K|\partial_x F_a| + K\sqrt{b}|\partial_x F_a|) = b(1 + \sqrt{b})K|\partial_x F_a| \\ &\leq b(1 + \sqrt{b})K(1 + r(y))f'_a(x). \end{aligned}$$

Hence

$$\frac{|w_2|}{|w_1|} \le \frac{b(1+\sqrt{b})K(1+r(y))f_a'(x)}{(1-r(y))(1-K\sqrt{b})f_a'(x)} = b\frac{(1+\sqrt{b})K(1+r(y))}{(1-r(y))(1-K\sqrt{b})}$$
$$\le b\frac{2^2K}{(1/2)^2} = 16Kb \le \sqrt{b},$$

if $b$ is chosen sufficiently small. □

This proposition tells us that we do not lose too much expansion to the $y$-direction under iterations. Hence we have an almost horizontal situation which can be treated as the one-dimensional case.

**Proposition 3.7** *Suppose that $DR_{a,b}$ induces a forward invariant cone field, $C(x,y) = \{(v_1,v_2) \in TN_{a,b}(x,y)\colon |v_2| \le \sqrt{b}|v_1|\}$. Set $(\xi_k,\eta_k) = DR^k_{a,b}(x,y)\cdot(1,0)$. For all $a \in (c, c+\epsilon)$ there exists $b_0 > 0$ such that for $b \in (0,b_0)$, there exists $\alpha > 0$ such that*

$$||(\xi_n,\eta_n)|| \ge \min\{e^\alpha, ||(\xi_1,\eta_1)||\}e^{(n-1)\alpha},$$

*for all $(x,y) \in N_{a,b}$ such that $R^k_{a,b}(x,y)) \notin S_{a,b}$ for $k = 0,...,n-1$.*

*Proof.* The proposition is obviously true for $n = 0$, so we assume that it is true for $n = k$. Set $w_k = (\xi_k,\eta_k)$. By our assumption, $|\eta_k| \le \sqrt{b}|\xi_k|$. Hence

$$||w_k||^2 = |\xi_k|^2 + |\eta_k|^2 \le (1+b)|\xi_k|^2,$$

so

$$|\xi_k|^2 \ge \frac{1}{1+b}||w_k||^2 \ge (1-b)||w_k||^2$$

for $b \in (0,1)$. By the definition of $DR_{a,b}$, we have

$$|\xi_{k+1}| = |\partial_x F_a(\xi_k,\eta_k)||\xi_k| \ge (1-r(\eta_k))f_a'(\xi_k)|\xi_k|.$$

Thus

$$||w_{k+1}|| \ge |\xi_{k+1}| \ge (1-r(\eta_k))f_a'(\xi_k)|\xi_k| \ge \sqrt{1-b}(1-r(\eta_k))f_a'(\xi_k)||w_k||.$$

By taking $b$ small enough we can find $\alpha > 0$ as in the one-dimensional proof (Proposition 2.11) . This $\alpha$ will be slightly smaller than the old one, but nevertheless, positive. □

**Corollary 3.8** *$R_{a,b}$ is Lyapunov chaotic on $\mathcal{A}_{a,b}$.*

*Proof.* For small $b$, $\mathcal{Z}_{a,b}$ consists of almost vertical line segments, whereas $\mathcal{A}_{a,b}$ is made up of almost horizontal components. This guarantees that, for sufficiently small $b$, the intersections of $\mathcal{Z}_{a,b}$ and $\mathcal{A}_{a,b}$ are transverse. Thus $\mathcal{A}_{a,b} \cap \mathcal{Z}_{a,b}$ will have measure zero in the sense of one-dimensional Lebesgue measure and all points in $\mathcal{A}_{a,b} \setminus \mathcal{Z}_{a,b}$ will have positive Lyapunov exponents by Proposition 3.7. □

**Corollary 3.9** *$\mathcal{Z}_{a,b}$ is dense in $\mathcal{A}_{a,b}$.*

The proof is identical to the one-dimensional case.

## 3.4 Topological Transitivity

What remains is to prove that $R_{a,b}$ is topologically transitive on $\mathcal{A}_{a,b}$. As in the one-dimensional case, we want to make sure that, at some stage of the iteration, a "good" domain is covered. By a good domain we here mean a connected set, $E \subset N_{a,b}$, such that we have

$$\pi_x(R_{a,b}(E)) \cap \pi_x(E) \ne \emptyset.$$

The two-dimensional case differs in the sense that iterates jump between pages of two Cantor books in a very complicated fashion, which is the reason why we have to study the $x$-projection.

**Proposition 3.10** *For all $a \in (c, c+\epsilon)$ there exists $b_0 > 0$ such that for $b \in (0, b_0)$, $R_{a,b}$ is topologically transitive on $\mathcal{A}_{a,b}$.*

*Proof.* Given two open sets $U$ and $V$ such that $U \cap \mathcal{A}_{a,b} \neq \emptyset$ and $V \cap \mathcal{A}_{a,b} \neq \emptyset$, we want to prove that there exists $n \geq 0$ such that $R^n_{a,b}(U) \cap V \neq \emptyset$. We may assume that $U$ and $V$ are balls centered on points in $\mathcal{A}_{a,b}$. Throughout the proof we will drop the parameters $a$ and $b$.

Let $N$ be the trapping region for $R$. Recall that $R(N)$ is contained in the interior of $N$. Thanks to the symmetry condition on $R$ (Definition 3.1(3)), $\{R^k(N)\}_{k=0}^{\infty}$ is a nested sequence of non-empty closed sets, so setting

$$\mathcal{A}^n = \cap_{k=0}^n R^k(N) = R^n(N),$$

we have $\mathcal{A} \subset \mathcal{A}^n$ for all $n \geq 0$. $R^k(N)$ consists of two Cantor books, each having $2^{k-1}$ pages. As $R$ is strongly contracting, the widths of the pages steadily decrease as $k$ grows. Hence, there exists $k_0 > 0$ such that all the pages of $\mathcal{A}^{k_0}$ have widths smaller than the radius of $V$. This means that at least one page of $\mathcal{A}^{k_0}$ will strictly slice $V$. This can happen in two ways, see Figure 8.

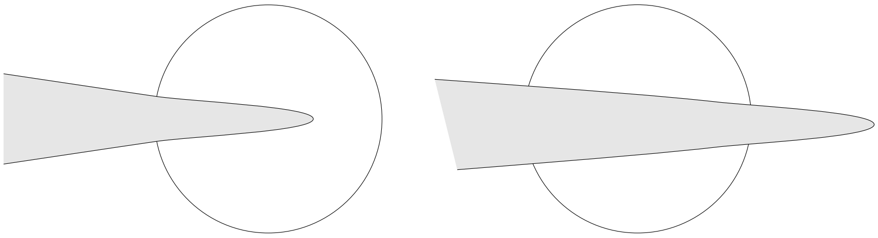

Figure 8: Two ways a page of the Cantor book can slice $V$.

Turning to $U$, we will assume that there exists $k_1 > 0$ such that $R^{k_1}(U)$ stretches horizontally across an "essential" half of one of the two components of $R(N)$. By an essential half, we mean a half that contains an image of the discontinuity, see Figure 9(a). If this is the case, $R^n(R^{k_1}(U))$ will, for large enough $n$, be included in each page of $R^{k_0}(N)$. This conclusion strongly depends on the fact that the iterates, $R^n(N)$, are nested. The pages of $R^n(R^{k_1}(U))$ will stretch horizontally across all pages of $R^{k_0}(N)$, except the two pages situated most outwardly, see Figure 9(b).

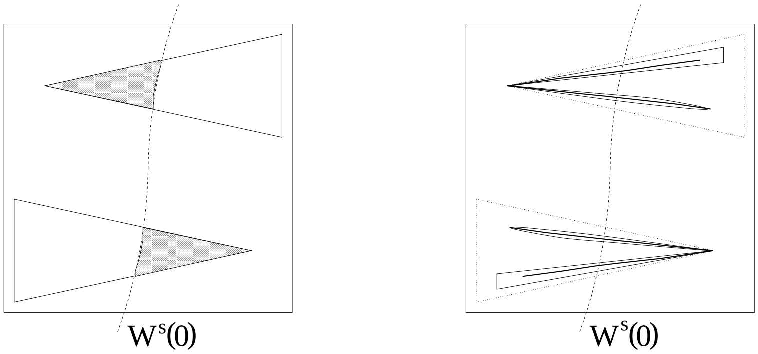


Figure 9: (a) The essential halves of $R(N)$, (b) Horizontally stretched iterates of $U$.

However, again due to the nesting, the pieces that are not reached in these two pages can not be contained in the attractor, and thus $V$ can not be centered around any point in these pieces. Hence the page of $R^{k_0}(N)$ that strictly slices $V$, contains a sufficiently long "sub page" of $R^n(R^{k_1}(U))$, so $R^{k_1+n}(U) \cap V \neq \emptyset$, see Figure 10. This proves the proposition.

We will now prove that our assumption on $U$ is correct if $b$ is chosen sufficiently small.

Assume that $U$ does not cover a good domain. By Proposition 3.7 we can, as in the one-dimensional case, arrange so that the largest component of $\pi_x(R^n(U))$ is more than doubled in length directly after it is sliced by the singularity, by taking $b$ sufficiently small. Hence $R^n(U)$ will eventually cover a good domain, i.e. there exists $k_2 \geq n$ such that

$$\pi_x(R^{k_2}(U)) \cap \pi_x(R^{k_2+1}(U)) \neq \emptyset.$$

This means that there exists $k_1 \geq k_2$ such that $R^{k_1}(U)$ is connected and stretches horizontally across an essential half of one of the two components of $R(N)$. This proves our assumption on $U$, and thus completes the proof. □

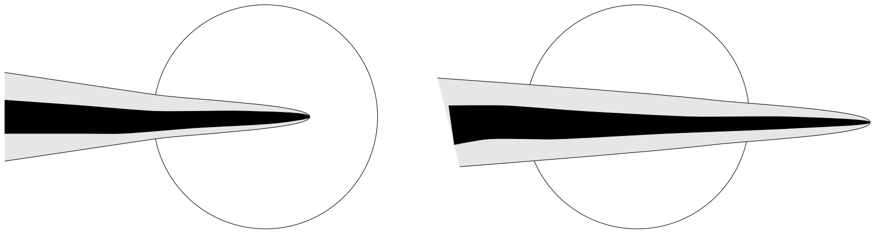

Figure 10: Two ways the page of $R^{k_0}(N)$ can strictly slice $V$.

**Acknowledgements:** I would like to thank the organizers of the International Workshop on Dynamical Systems and Geometry held at PUC (Pontifícia Universidade Católica), and everyone at IMPA (Instituto de Matemática Pura e Aplicada) for their warm hospitality during my stay in Rio, Brazil. Both departments provided financial support and excellent working conditions during the completion of this paper. Many thanks also to Lennart Carleson for being such an inspiring supervisor. Finally, I thank Johan Steensland for proof-reading large parts of the manuscript.

# References


[1] M. Benedicks, L. Carleson, *The Dynamics of the Hénon Map*, 73-169, Ann. of Math. **133**, 1991

[2] G.R. Belitskii, *Equivalence and Normal Forms of Germs of Smooth Mappings*, 107-177, Russ. Math. Surv. **33**, 1978

[3] P. Glendinning, *Stability, Instability and Chaos*, Cambridge Texts in Applied Mathematics, 1994

[4] J. Guckenheimer, R. F. Williams, *Structural Stability of Lorenz Attractors*, 307-320, Publ. Math. **50**, 1979

[5] S.P. Hasting, W.C. Troy, *A Shooting Approach to the Lorenz Equations*, 298-303, Bull. Amer. Math. Soc. **27**, 1992

[6] E.N. Lorenz, *Deterministic Non-periodic Flows*, 130-141, J. Atmos. Sci. **20**, 1963

[7] S. Luzzatto, M. Viana, *Positive Lyapunov Exponents for Lorenz-like Families with Criticalities*, Preprint, 1995

[8] K. Mischaikow, M. Mrozek, *Chaos in the Lorenz Equations: A Computer-Assisted Proof*, 66-72, Bull. Amer. Math. Soc. **32**, 1995

[9] E. Nelson, *Topics in Dynamics I: Flows*, Princeton Univerity Press, 1964

[10] J. Palis, F. Takens, *Hyperbolicity & Sensitive Chaotic Dynamics at Homoclinic Bifurcations*, Cambridge Studies in Advanced Mathematics, 1993

[11] D. Rand, *The Topological Classification of Lorenz Attractors*, 451-460, Math. Proc. Camb. Phil. Soc. **83**, 1978

[12] K. A. Robbins, *Periodic Solutions and Bifurcation Structure at High r in the Lorenz Model*, 457-472, Siam. J. Appl. Math. **36**, 1979

[13] C. Robinson, *Homoclinic Bifurcation to a Transitive Attractor of Lorenz Type*, 495-518, Nonlinearity **2**, 1989

[14] W. Tucker, *Transitivity of Lorenz-like Maps and the Tired Baker's Map*, in preparation

[15] R. F. Williams, *The Structure of Lorenz Attractors*, 321-347, Publ. Math. **50**, 1979



*Address:* Warwick Tucker
Department of Mathematics
Uppsala University, Box 480
S-751 06 Uppsala
Sweden

*E-mail:* `warwick@math.uu.se`